HOW LARGE IS THE SUN'S TOTAL MAGNETIC FLUX?

N. A. Krivova[1,2], S. K. Solanki[1], and M. Fligge[3]

[1]Max-Planck-Institute for Aeronomy, 37191 Katlenburg-Lindau, Germany
[2]On leave from Astronomical Institute, St. Petersburg University, 198504 St. Petersburg, Russia
[3]Institute of Astronomy, ETH Zentrum, CH-8092 Zürich, Switzerland

ABSTRACT

Variations in the radiative output of the Sun are directly allied to changes in the amount and distribution of solar surface magnetic field. The variability of solar irradiance on time-scales significantly shorter than a solar cycle can be produced by the spatial and temporal evolution of active regions, whereas its secular variations ensue from changes of the quiet-Sun magnetic flux on longer time-scales. The relative amounts of the magnetic flux in active regions and in the quiet Sun as well as their cyclic evolution have been studied by Harvey (1994) on the basis of the NSO/Kitt Peak synoptic maps. Since a single pixel of such a map is much bigger than individual small-scale magnetic elements and opposite polarities may be present within the same pixel, some magnetic flux went uncounted, so that the flux obtained by Harvey (1994) represents a lower limit to the true amount of magnetic flux present on the Sun. We use MDI full-disc and high-resolution magnetograms to estimate the total magnetic flux of the Sun.

Key words: Sun: activity; Sun: magnetic fields; Sun: variability.

1. INTRODUCTION

The total solar irradiance believed to be constant until recent satellite measurements proved to vary at all observable time-scales (Willson & Hudson, 1988, 1991; Fröhlich & Lean, 1998; Fröhlich, 2000). This variability, so weak that it went unnoticed up to nearly the end of the 20th century, may affect the Earth's climate (e.g. Lean et al., 1995; Solanki & Fligge, 1998, 1999). The solar radiative output mirrors changes in solar magnetic activity. Spatial and temporal evolution of active regions causes irradiance variations on time-scales of days to a solar cycle (with some contributions also from the network). Of even greater importance for the Earth is a possible secular trend in the irradiance variability, caused by changes in the quiet-Sun magnetic field. A detailed understanding of the evolution of the solar surface magnetic field is, therefore, crucial for understanding of the variability of the solar irradiance and probably the Earth's climate.

Harvey (1994) followed the evolution of the magnetic field in active regions and in the quiet Sun during a solar cycle using NSO/Kitt Peak (KP) synoptic charts. The magnetic field in the quiet Sun dominates during a solar activity minimum and shows little variation on a time-scale of a solar cycle. At activity maximum active regions play the main role and their total magnetic flux ,$\Phi_{\rm AR}$, exceeds by up to a factor of 3 the flux in the quiet Sun, $\Phi_{\rm QS}$. However, the estimated magnetic flux turns out to be markedly dependent on the spatial resolution of the analysed magnetograms (Krivova et al., 2002). Since small magnetic elements are often much smaller than the size of a pixel in the KP synoptic charts and elements of opposite polarities can be present within the same pixel, the total magnetic flux, especially in the quiet Sun, is strongly underestimated.

We use full-disc magnetograms recorded by MDI (Michelson Doppler Interferometer on board SOHO) to estimate the total magnetic flux of the Sun and to compare it with the results on the basis of the KP synoptic charts (Sects. 2 and 3). Following Harvey (1994), we consider active regions and the quiet Sun individually. We also check, how much flux may still be hidden within the 'very' quiet Sun, at a signal level comparable to the noise in the MDI magnetograms (Sect. 4).

2. METHOD

We analyse synoptic charts for the Carrington Rotation 1975 (April–May 2001) created from MDI full-disc magnetograms. The noise (1σ) in the original MDI magnetograms obtained with a 1-minute cadence is typically about 20 G (Scherrer et al. 1995; see also Ortiz et al. 2002 and Sect. 4). This is comparable to the magnetic signal from the quiet Sun. To reduce the noise level, we sum up 5, 20 or 56 individual magnetograms ($\sigma \approx 9$ G, 4.5 G and 2.7 G,

Proc. 'SOLMAG: Magnetic Coupling of the Solar Atmosphere Euroconference and IAU Colloquium 188'
Santorini, Greece, 11-15 June 2002 (ESA SP-505, October 2002)

Table 1. Magnetic flux, Φ_{MDI}, of synoptic maps created from MDI full-disc magnetograms, normalised to the flux, which would be measured for these maps with the KP synoptic charts resolution, $\Phi_{KP,\,SC}$. Total flux and flux from quiet Sun (QS) and active regions (AR) are listed separately. The rotation maps were made using original 1-minute magnetograms, as well as 5-, 20- and 56-minute averages. Signal below 1σ, 2σ or 3σ was assumed to be noise in the three considered cases, respectively.

	1-min (σ = 20G)	5-min (σ = 9G)			20-min (σ = 4.5G)			56-min (σ = 2.7G)		
	1σ	1σ	2σ	3σ	1σ	2σ	3σ	1σ	2σ	3σ
AR+QS	1.38	1.30	1.12	1.05	1.25	1.15	1.09	1.22	1.15	1.10
AR	1.05	1.04	1.03	1.03	1.05	1.04	1.03	1.04	1.04	1.03
QS	1.97	1.75	1.31	1.10	1.60	1.36	1.21	1.50	1.35	1.23

respectively). Solar differential rotation is taken into account. Signal within $[-1\sigma; +1\sigma]$ is set to 0. Since in this case a considerable amount of noise is identified as magnetic signal, we also use 2σ and 3σ thresholds. Unfortunately, a lot of real signal vanishes, too, in particular for the higher thresholds and the 1- and 5-minute averages.

The low-noise 20- and 56-minute averages can, unfortunately, not be produced for the period of minimum activity, since magnetograms were not recorded regularly enough. Another problem with these low-noise maps is that magnetic features evolve in the course of an hour and the peculiar motion of magnetic features can move them out of a given pixel in this time. This means that in these averaged magnetograms the magnetic signal is smeared and thus further reduced, partly because some of it falls below the noise limit, partly due to cancellation.

Finally, active regions are separated from the quiet Sun following Harvey (1994). Every running box of 20×20 pixels within the synoptic chart is examined for the amplitude of the variation of the magnetic field: stronger field variations are typical of active regions. About 10% of all pixels for CR 1975 fall within the active regions.

To compare the obtained synoptic charts with those having KP synoptic chart resolution, we bin subarrays of 9×6 pixels together (see Harvey, 1994; Scherrer et al., 1995). Active regions are isolated in these new, low-resolution maps too and the threshold between the active and quite Sun is adjusted to give the same relative areas for both components as in the high resolution synoptic charts.

3. RESULTS

The ratios of the total flux obtained for the two resolutions are given in Table 1 (hereafter, index 'KP, SC' refers to maps/magnetograms obtained from MDI data by reducing their spatial resolution to that of the Kitt Peak synoptic charts). The results for different integration times and noise thresholds (1, 2 and 3σ) are listed. Thresholding at 2σ and 3σ (20 and 40G) for 1-minute maps carries almost no information, since practically all small-scale magnetic elements are eliminated in this way.

It is immediately obvious that the spatial resolution is rather unimportant for determining the total magnetic flux of active regions: the 'missing' flux (i.e. the flux not seen in the Kitt Peak synoptic charts, but present in the MDI magnetograms) is less than 5%, whereas it is far more important for the quiet Sun.

This is also evidenced by Fig. 1. Here, we have cut the CR 1975 synoptic chart obtained from magnetograms averaged over 56 minutes into 28 vertical strips, each corresponding to one day. We have then found the ratio $\Phi_{MDI}/\Phi_{KP,\,SC}$ for the total flux, quiet Sun and active regions for every strip and plotted them versus the corresponding Φ_{MDI}. The ratios for the total flux are shown by asterisks, whereas diamonds and plus signs represent the quiet and active Sun, respectively. Ratios for active regions all lie close to 1. The reason is that active regions are more uniform than the quiet Sun network, in the sense that the former contain larger unipolar patches, usually bigger than a pixel in the KP synoptic chart. The ratios grow quickly with decreasing magnetic flux — the effect of the resolution becomes more and more important with decreasing activity level, when small magnetic elements start playing a leading role. For the most quiet regions, $\Phi_{MDI}/\Phi_{KP,\,SC}$ reaches 1.6–1.65 with the 1σ noise threshold.

Since with 3σ almost all the noise must have been eliminated, the 56-minute average at 3σ provides the absolute lower limit for the ratio: at least 20% of the quiet-Sun flux is still hidden at the KP synoptic chart resolution (Table 1 and Fig. 2). This limit may, however, be too conservative, and the real ratio is likely to lie between those obtained for the 56-min averages at 1σ and 2σ. This is suggested by a comparison of fluxes obtained for the rotation maps with different integration time (or noise level) and noise threshold. At 1σ, the flux Φ_{MDI} decreases from 1-minute to 56-minute averages, suggesting that there is still a lot of noise in 1- and 5-minute data, which goes down with integration time. Already at 2σ the

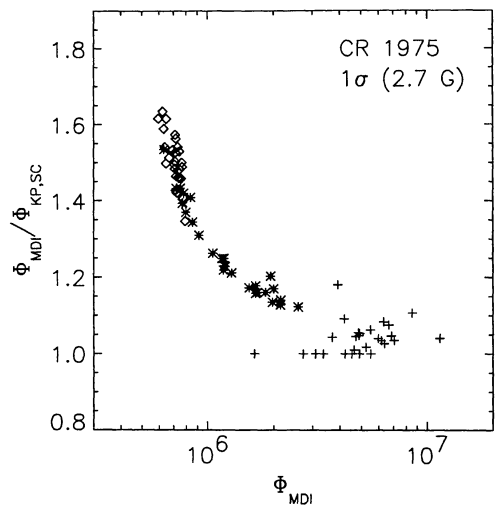

Figure 1. Dependence of the $\Phi_{MDI}/\Phi_{KP,\,SC}$ ratio on the total magnetic flux within a longitude band (see text for details). The noise threshold has been set at 1σ. Asterisks: total flux; pluses: active areas only; diamonds: quiet Sun only.

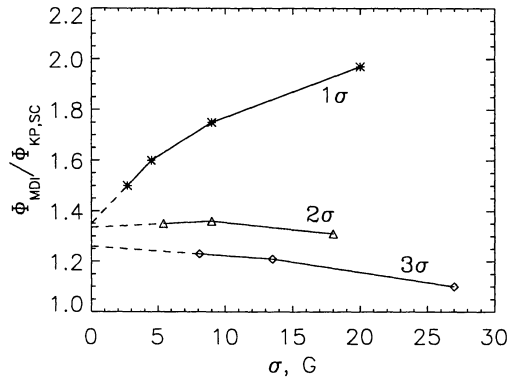

Figure 2. Dependence of the $\Phi_{MDI}/\Phi_{KP,\,SC}$ ratio on the noise level (i.e. total integration time) of magnetograms at 1σ, 2σ and 3σ. Quiet-Sun component is shown. Dashed lines are linear extrapolations to the '0'-noise level.

situation reverses: the flux increases with integration time, which implies that now we see more and more weak features as the noise level is reduced and this effect overrides the decrease in the apparent signal due to lower noise. In Fig. 2, the quiet-Sun ratios $\Phi_{MDI}/\Phi_{KP,\,SC}$ obtained with different thresholds are shown versus the noise level of magnetograms. Linear extrapolations of the curves at 1σ and 2σ to 0 G yield a very similar value of about 1.34, while an extrapolation of the 3σ provides a somewhat lower ratio of 1.26.

In the next section another, independent method is used to compare different thresholds.

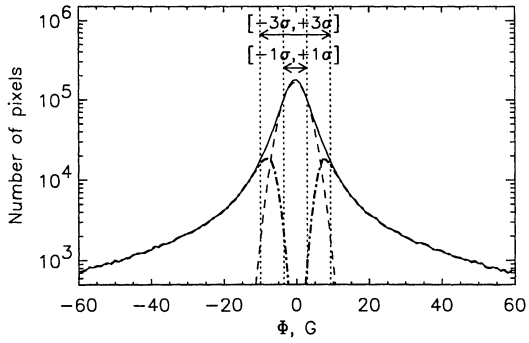

Figure 3. Histogram (solid) of the magnetic signal Φ for the CR 1975 synoptic chart (56-minute average). Dashed: a Gaussian fit representing the noise distribution (see text); dot-dashed: difference between the histogram of the total signal and the Gaussian. Vertical dotted lines and the arrows show the $\pm1\sigma$ and $\pm3\sigma$ intervals, where σ is the width parameter of the Gaussian.

4. MAGNETOGRAM SIGNAL HIDDEN IN NOISE

Let us now estimate the amount of weak signal which may still be hidden within the noise. We use the synoptic chart obtained from 56-minute averages and construct a histogram of the magnetic signal (again for the total flux, quiet Sun and active regions individually). The core part of the histogram for the total magnetic flux is shown in Fig. 3 (solid line). We have only included pixels with $\mu > 0.8$. Since noise is randomly distributed over the pixels, it is expected to have a Gaussian distribution centred at 0 G. The histogram, indeed, appears to be similar to a Gaussian in its central part.

We now *assume* that magnetic signal in the core of the histogram is mainly due to noise. To represent this noise, we fit a Gaussian, $\mathcal{G}$, to the histogram, $\mathcal{H}$, in such a way that it never exceeds $\mathcal{H}$, since signal from noise cannot exceed the total registered signal (dashed line in Fig. 3). Now, the difference between $\mathcal{H}$ and $\mathcal{G}$ (dot-dashed) gives the distribution of the real solar signal and its integral over all pixels yields an estimate of the actual magnetic flux.

Most probably, a part of the signal falling within the fitted Gaussian is also real. One indication for this is that the value of σ we obtain as the half width at half heigth of $\mathcal{G}$ is somewhat higher (3.2 G) than the expected value for 56-minute averages ($\lesssim 20/\sqrt{56} \approx$ 2.7 G). Note, that for 1-minute magnetograms our fitted Gaussians indeed give $\sigma \lesssim 20$ G. Furthermore, we make the conservative assumption that at small values of Φ only noise is present. This leads to the very steep and possibly artificial decrease of the dot-dashed curve in Fig. 3 near $\Phi = 0$. Therefore, the magnetic flux we find in such a way represents a lower limit only.

In Table 2 we compare the total amount of flux for pixels with $\mu > 0.8$ deduced from $\mathcal{H} - \mathcal{G}$ with the amount obtained by setting a threshold (Sect. 3). In columns 2–4 the ratios of the fluxes deduced from the two techniques are listed. The ratio is close to unity for 1σ and steadily increases as one takes larger thresholds up to 3σ. This is not surprising and only says that we are missing increasing amounts of magnetic flux when going to a higher threshold. Also not surprising is the fact that the ratio $(\mathcal{H}-\mathcal{G})/\Phi_{\rm MDI}(\Theta)$ increases most rapidly for the quiet Sun, where we expect the flux to be weakest. We expect that much of this hidden flux is due to intranetwork fields. It is clear that taking 1σ for the noise threshold, we indeed may count some noise as the solar magnetic flux, although this false signal is quite low, less than a few percent (remember that the ratios in Table 2 are lower limits). We stress here that this does not imply that all the points lying above 1σ are real signal; only that the amount of flux hidden below 1σ is approximately equal to the contribution from noise above 1σ. With the 2σ cut-off we have lost at least 15% of the actual flux in the quiet Sun and even more than 30% with 3σ.

In column 5 we again list the ratio of the flux deduced from the MDI synoptic chart compared with the synoptic chart at Kitt Peak resolution. The listed $\Phi_{\rm MDI}/\Phi_{\rm KP,\,SC}$ values are for the 56-min averages (see Table 1). In order to obtain an improved estimate of the flux missed in KP synoptic charts we need to multiply $(\mathcal{H}-\mathcal{G})/\Phi_{\rm MDI}$ (which is an indicator of the fraction of the flux hidden in the noise of MDI magnetograms) with $\Phi_{\rm MDI}/\Phi_{\rm KP,\,SC}$. This product, listed in the last column of Table 2, gives our final estimates of the total flux found with the MDI data with respect to the flux obtained with the KP synoptic chart resolution. Encourangingly, these final numbers depend only weakly on the threshold Θ. The numbers imply that at least 50% of the quiet-Sun magnetic flux went uncounted in KP synoptic charts.

Table 2. Ratios (columns 2–4) of the magnetic flux of the CR 1975 synoptic map (56-min) obtained by two different methods, $\Phi_{\rm MDI}$ and $\mathcal{H}-\mathcal{G}$ (Sects. 3 and 4, respectively) for different thresholds, Θ, (column 1). The 5th column lists the $\Phi_{\rm MDI}/\Phi_{\rm KP,\,SC}$ ratios for the quiet Sun found in Sect. 3 (Table 1) and the last column is the product of columns 4 and 5, suggesting final estimates of the total magnetic flux in the MDI vs. KP synoptic charts.

Θ	$\frac{\mathcal{H}-\mathcal{G}}{\Phi_{\rm MDI}}$			$\frac{\Phi_{\rm MDI}}{\Phi_{\rm KP,\,SC}}$	$\frac{\mathcal{H}-\mathcal{G}}{\Phi_{\rm KP,\,SC}}$
	AR+QS	AR	QS	QS	QS
1σ	0.99	1.00	0.97	1.50	1.46
1.5σ	1.02	1.00	1.06		
2σ	1.05	1.01	1.15	1.35	1.55
3σ	1.10	1.02	1.32	1.23	1.62

5. CONCLUSION

Using KP synoptic charts, Harvey (1994) found that the total magnetic flux in active regions at activity maximum is about 3 times higher than the flux at activity minimum. The spatial resolution of these data was, however, insufficient to resolve small magnetic elements comprising the quiet Sun. We use MDI full-disc magnetograms to estimate the total magnetic flux and to compare it to the resolution of KP synoptic charts. The analysis has been carried out separately for the Sun as a whole, quiet Sun and active regions. Whereas for active regions, the effect of the spatial resolution is rather unimportant, significant magnetic flux contained in small-scale magnetic elements goes uncounted because opposite polarities are present within a single resolution element of the Kitt Peak synoptic charts.

Compared to the full-disc resolution of MDI, at least 50% of the quiet-Sun flux escapes notice in KP synoptic charts. This means that the ratio $\Phi_{\rm AR}/\Phi_{\rm QS}$ is, in fact, distinctly lower than is found from the KP data.

Furthermore, our analysis involving high-resolution MDI magnetograms (Krivova et al., 2002) suggests, that even the resolution of the full-disc MDI data is insufficient to resolve all weak magnetic elements. Up to a factor of 2 more flux (but at least 20%) can still be hidden within the full-disc resolution data when compared to the high-resolution mode. When taken together with the results presented here this suggests that only approximately half of the magnetic flux in the quiet Sun is visible in Kitt Peak synoptic charts.

REFERENCES

Fröhlich C., 2000, Sp. Sci. Rev., 94, 15

Fröhlich C., Lean J., 1998, GRL, 25, 4377

Harvey K.L., 1994, In: Pap J.M., Fröhlich C., Hudson H.S., Solanki S.K. (eds.) IAU Coll. 143: The Sun as a Variable Star, 217–225, Cambridge Univ. Press

Krivova N.A., Solanki S.K., Fligge M., 2002, SOHO-11, ESA-SP, 508, in press

Lean J., Beer J., Bradley R., 1995, GRL, 22, 3195

Ortiz A., Solanki S.K., Domingo V., Fligge M., Sanahuja B., 2002, A&A, in press

Scherrer P.H., Bogart R.S., Bush R.I., et al., 1995, Solar Physics, 162, 129

Solanki S.K., Fligge M., 1998, GRL, 25, 341

Solanki S.K., Fligge M., 1999, GRL, 26, 2465

Willson R.C., Hudson H.S., 1988, Nature, 332, 810

Willson R.C., Hudson H.S., 1991, Nature, 351, 42